Journal of King Saud University – Science (2013) 25, 149–155

King Saud University

Journal of King Saud University – Science

www.ksu.edu.sa

www.sciencedirect.com

ORIGINAL ARTICLE

Characterization of kaolin intercalates of oleochemicals derived from rubber seed (*Hevea brasiliensis*) and tea seed (*Camelia sinensis*) oils

Chinedum O. Mgbemena [a,*], Naboth O. Ibekwe [b], Rugmini Sukumar [c], A.R. Ravindranatha Menon [c,*]

[a] *National Engineering Design Development Institute, Nnewi, Nigeria*

[b] *Department of Mechanical Engineering, Nnamdi Azikiwe University, Awka, Nigeria*

[c] *National Institute for Interdisciplinary Science and Technology, Thiruvananthapuram 695019, India*

Received 28 August 2012; accepted 28 November 2012

Available online 27 December 2012

KEYWORDS

BET surface;
BJH adsorption;
Kaolin;
Langmuir surface;
Rubber seed oil;
Tea seed oil

Abstract Kaolin intercalates were prepared by employing derivatives of oleochemicals namely rubber seed oil (SRSO) and tea seed oil (STSO) and characterized by employing powder X-ray diffraction (PXRD), Fourier transform infrared spectroscopy (FTIR) and nitrogen adsorption–desorption (NAD) techniques. Intercalation was achieved in the presence of hydrazine hydrate as co-intercalate. The PXRD patterns showed an increase in the interlayer basal spacing d_{001} for the SRSO treated and STSO treated kaolins confirming intercalation process. The FTIR studies indicated that the fatty acid salts of rubber seed oil and tea seed oil were effectively intercalated in the kaolinite layers as per the bands at 1564 cm^{-1} and 1553 cm^{-1} for SRSO treated and STSO treated kaolinites, respectively. The SEM revealed intercalation of organic materials in the kaolinite layers. The NAD results showed that intercalation of kaolin resulted in an overall decrease in the specific surface area as well as pore volume. Specific surface area decreased in

* Corresponding authors. Tel.: +234 7034308877 (C.O. Mgbemena), +91 9495813059 (A.R.R. Menon).

E-mail addresses: edumgbemena@yahoo.com (C.O. Mgbemena), ravindranathamenon@yahoo.co.in (A.R. Ravindranatha Menon).

Peer review under responsibility of King Saud University.

doi:10.1016/j.jksus.2012.11.004

Production and hosting by Elsevier

the following order: untreated (pristine) kaolin > STSO treated kaolin > SRSO treated kaolin and pore size in the order: untreated (pristine) kaolin > SRSO treated kaolin > STSO treated kaolin.

1. Introduction

Kaolin commonly called China clay is a ubiquitous mineral which consists mainly of the mineral kaolinite having an empirical formula of $Al_2Si_2O_5(OH)_4$ and theoretical chemical composition as follows: Si_2 = 46.54%; Al_2Si_2 = 39.50%; and H_2O = 13.96% with structure consisting of silicon oxide tetrahedral and gibbsite octahedral sheets typical of type 1:1 minerals. They can be employed in many applications for property enhancements; for example in ceramics, medicine, paper coatings, as a food additive, in toothpaste, as a light diffusing material in white incandescent light bulbs, and in cosmetics. It is generally the main component in porcelain. It is also used in paint production to extend titanium dioxide (TiO_2) and modify gloss levels; in rubber for semi-reinforcing properties; and in adhesives to modify rheology (Krishnan et al., 2012; Guessoum et al., 2012; Preetha and Rani, 2012; Songfang et al., 2011; Ma and Bruckard, 2010; Murray, 2007; Ciullo, 1996).

Kaolin is naturally hydrophilic and is not best suited for some applications like in Natural Rubber (NR) reinforcement due to the hydrophobicity of Natural Rubber. To ensure compatibility with the NR matrix, kaolin is organomodified by intercalation with some organic molecules.

Most materials used as organomodifiers are obtained from petroleum or natural gas and these are very expensive due to the non-renewable nature of their sources. Oleochemicals are preferred as kaolin organomodifiers based on their renewable and inexhaustible nature, availability, eco-friendliness and conformability.

Nitrogen gas adsorption or the Brunauer–Emmett–Teller (BET) method is a proven method for the characterization of a wide range of mesoporous materials including kaolin (Wang et al., 2011; Sing, 2001; Reichenauer and Scherer, 2001; Inel and Tumsek, 2000). The adsorption and desorption isotherms provide practicable information about materials that can be applied into the specific surface area, the pore size and pore volume.

Following the pioneering work of Irving Langmuir in 1918, the interpretation of adsorption data became interesting. Many further attempts have been made to interpret the isotherm information, including BET and Barrett–Joyner–Halenda (BJH). BET is a standard method of determining the surface area. Owing to the artificial nature of the BET theory the range of applicability of the BET equation is always limited to a part of the nitrogen isotherm in the order $0.05 < P/P_0 < 0.30$. By measuring the volume of gas adsorbed at a particular partial pressure, the Brunauer–Emmett–Teller (BET) equation gives the specific surface area of the material.

The classification of pores according to size has been proposed by the International Union of Pure and Applied Chemistry as follows: micropore is defined as pores with an internal width less than 2 nm; mesopore for pores between 2 and 50 nm and macropore for pores greater than 50 nm. Pore types and pore sizes play important roles in the adsorption process. Different methods are employed to determine the pore size and the pore size distribution.

The aim of this study is to evaluate and compare the characteristics of kaolin and its derived modified forms resulting in partial intercalation as well as delamination or exfoliation. All the samples were analyzed with respect to a specific surface area by Single point surface area, BET surface area, Langmuir surface area, BJH Adsorption cumulative surface area, pore volume and size by BJH Adsorption cumulative pore volume and BJH cumulative average pore diameter, respectively. The SRSO treated kaolin and STSO treated kaolin were initially characterized by Powder X-ray Diffraction (PXRD) and Fourier Transform Infrared spectroscopy (FTIR) to verify intercalation of the organic substance within the kaolinite layers.

2. Experimental

2.1. Materials

BCK grade Kaolin used in this work was obtained from English Indian Clays Ltd. Thiruvananthapuram, India; Rubber seed oil (RSO) and Tea seed oil (TSO) were provided by NIIST, CSIR, Thiruvananthapuram, India; Laboratory grades of Sodium hydroxide (MERCK) and Hydrazine hydrate (FINNAR) were obtained from local suppliers.

2.2. RSO-Kaolin treatment

Following a similar procedure earlier reported by Rugmini and Menon (2008) the sodium salt of rubber seed oil (SRSO) was stoichiometrically prepared by mixing 33 mL of RSO with 100 mL of 20% NaOH solution in an ice bath with continuous stirring for 12 h. The resulting mixture was kept for 1 day to cure. The final pH of the resulting solution was adjusted to 9. The SRSO was washed with water to remove excess of NaOH, dried in a hot air oven and the dried product was powdered. This was followed by slowly adding 98 g of Kaolin to a mixture containing 20 g SRSO and 70 mL hydrazine hydrate with vigorous stirring at 20 °C. The mixture was homogenized using an Art-MICCRA D-8 (Germany) homogenizer, and the sample was dried in a freeze drier.

2.3. TSO-Kaolin treatment

Sodium salt of tea seed oil (STSO) was stoichiometrically prepared by reacting 28 mL of TSO with 27 mL of 20% NaOH solution in an ice bath with constant stirring for 12 h and kept for 1 day to allow for curing to take place. The pH of the resulting solution was adjusted to 9. STSO was washed with water to remove excess base; dried in a hot air oven to remove residual moisture and powdered. Then 98 g of Kaolin was slowly added to a mixture containing 20 g STSO and 70 mL

hydrazine hydrate with vigorous stirring at 20 °C. The mixture was homogenized using an Art-MICCRA D-8 (Germany) homogenizer, and the sample was dried in a freeze drier.

2.4. Characterization of the untreated and treated Kaolins

2.4.1. Scanning electron microscopy

The morphology of the pristine and treated Kaolin was observed from the JEOL (JSM- 5600LV SEM) at an acceleration voltage of 15 kv. The image magnification of ×15,000 was selected to reveal the kaolinite layers. The samples to be examined were initially surface coated using palladium–gold plating by sputtering to increase conductivity.

2.4.2. X-ray diffraction

PXRD of the samples was performed using a PHILIPS-1710 X-ray diffractometer using monochromatic Ni-filtered Cu Kα radiation 1.5418 Å at 40 kV and 20 mA from $2\theta = 5$–55° with a speed of 2°/min and step size of 0.05°. The diffraction of X-rays by crystals is described by Bragg's Law:

$$n\lambda = 2d\sin\theta$$

where λ is the wavelength of monochromatic X-ray source measured in Angstrom (Å), "d" is the interplanar spacing generating the diffraction measured in Angstrom, θ is the diffraction angle at which X-ray falls on the sample, and n is the order of reflection.

2.4.3. FTIR

The FTIR spectra of the organomodified and untreated kaolins were obtained using MAGNA 560 NICOLET Fourier Transform Infrared spectrometer. Wavenumbers from 3800 cm^{-1} to 600 cm^{-1} were considered.

2.4.4. NAD (BET Test)

NAD experiment was performed using the GEMINI DEVICE (Gemini 2375 V5.01, Micromeritrics Corporation, USA). A known amount (~3–4 mg) of the sample was weighed and degassed at 120 °C under vacuum (780 mmHg) to remove adsorbed gases and moisture. The material is again weighed and subjected to nitrogen adsorption under vacuum and liquid nitrogen conditions. The adsorption and desorption information obtained from each run was used to determine the specific surface area (m^2/g), pore size distribution and pore size (nm) using the BET and BJH models. The specific surface area was calculated using the BET method from the adsorption isotherm within the relative pressure ($P = P_0$) range 0–0.375. The

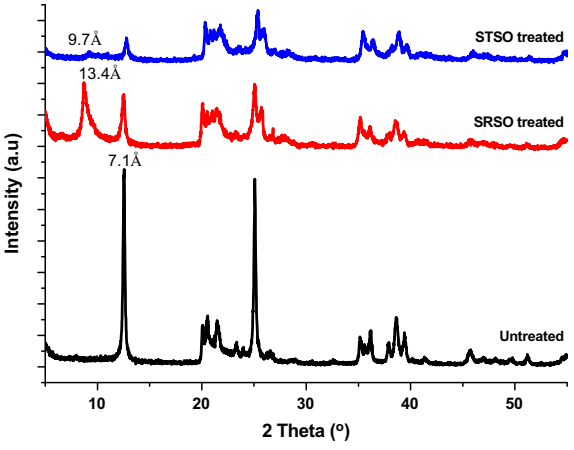

Figure 1 Combined X-ray diffraction pattern for pristine kaolin, SRSO treated kaolin and STSO treated kaolin.

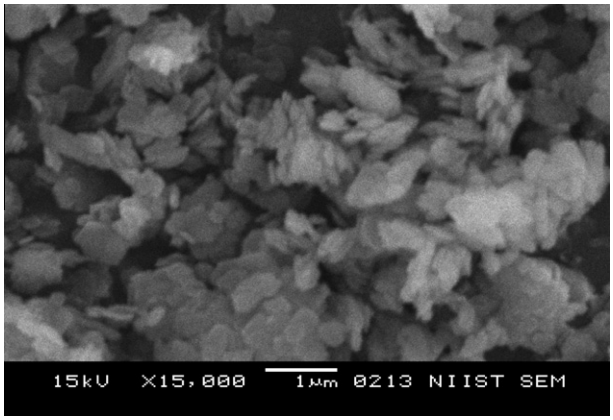

Figure 2 Pristine Kaolin at a magnification of ×15,000.

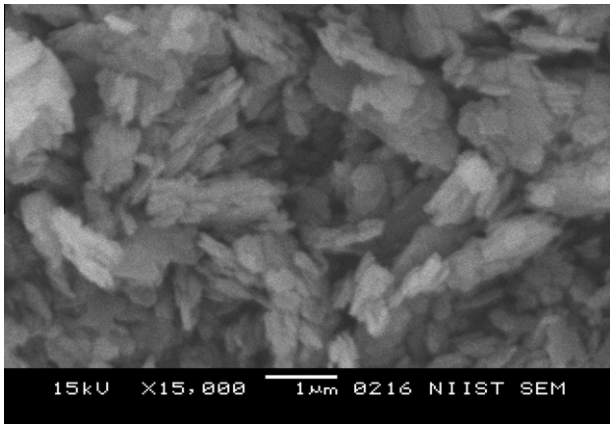

Figure 3 SRSO treated Kaolin at a magnification of ×15,000.

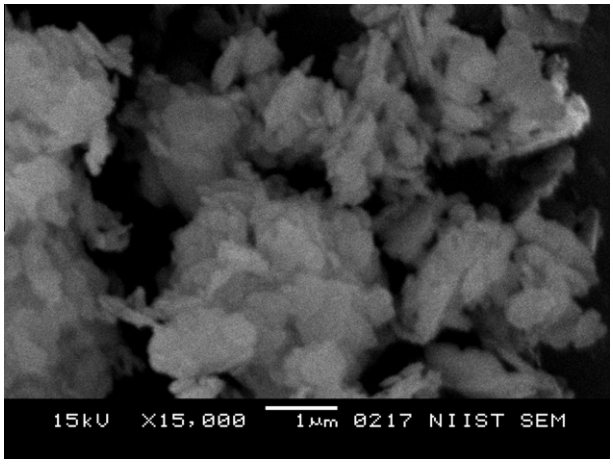

Figure 4 STSO treated Kaolin at a magnification of ×15,000.

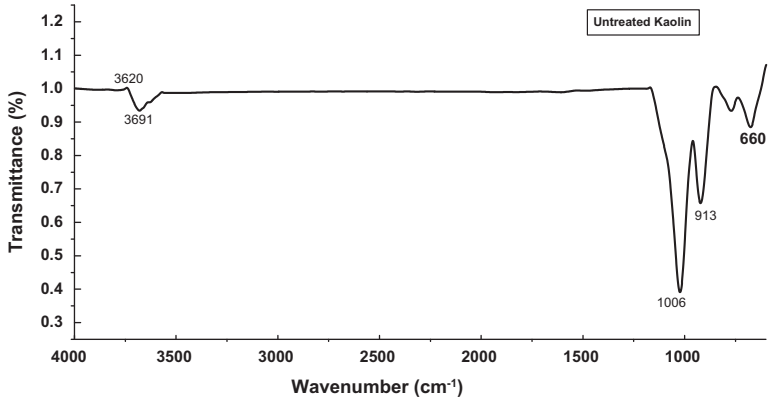

Figure 5 FTIR spectra for untreated Kaolin.

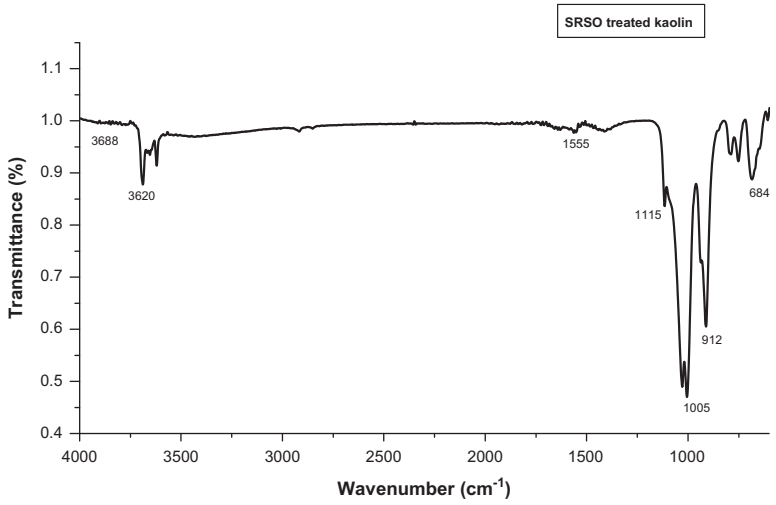

Figure 6 FTIR spectra for SRSO treated Kaolin.

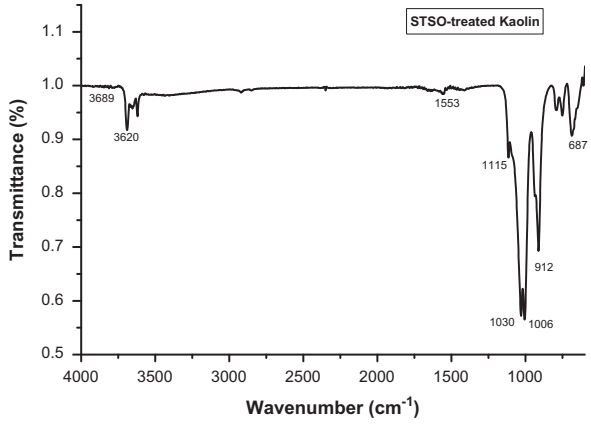

Figure 7 FTIR spectra for STSO treated Kaolin.

nitrogen molecule covers an area of 16.2 Å^2 ($\equiv$0.162 nm^2). Adsorption measurements can estimate the porous volume corresponding to $P/P_0 = 1$. The pore size distribution in the mesoporous range (2–50 nm) was evaluated according to the BJH method. This experiment was conducted for the untreated, SRSO treated and STSO treated kaolins, respectively.

3. Results and discussion

3.1. X-ray diffraction studies for the Kaolin

The X-ray diffraction patterns of the untreated and treated Kaolins are shown in Fig. 1. It is evident that all the samples exhibited a diffraction peak at $2\theta = 12.54°$ which is assigned to the characteristic interlayer basal spacing d_{-001} of kaolinite at 7.10 Å. A closer value of 7.15 Å was obtained by Rugmini and Menon (2008) for untreated kaolin. However, the intensity of the peak has reduced significantly in the case of its organo-modified forms indicating partial modification (intercalation or delamination or exfoliation). In the SRSO treated Kaolin, a displacement of the peak to lower angles $2\theta = 6.60°$ has taken place resulting in an interlayer basal spacing d_{-001} of 13.40 Å. The STSO treated Kaolin recorded a much lower interlayer basal spacing of d_{-001} of 9.70 Å at angle $2\theta = 9.13°$ compared to the SRSO treated Kaolin. Both the patterns thus indicated that the kaolinite interlayer region has expanded, along the *c*-axis, as a result of the intercalation of the oleo derivatives achieved by employing hydrazine hydrate as co-intercalate. However, it was difficult to differentiate between intercalation, delamination and exfoliation. The value obtained for STSO treated kaolin in this work was much

Table 1 Position and assignment of the various absorption bands in the FTIR spectra of the Kaolin and its treated forms.

Position and assignment of bands (cm^{-1})	Kaolin	SRSO-treated Kaolin	STSO-treated Kaolin
STSO-treated Kaolin			
OH stretching of inner surface hydroxyl groups (in plane vibration with a transition moment nearly perpendicular to the (0 0 1) plane)	3691	3688	3689
OH stretching of inner surface hydroxyl groups (anti-phase vibration with a transition moment lying in the (0 0 1) plane)	3655	3654	3654
OH stretching of inner surface hydroxyl groups	3620	3620	3620
C═O stretching (indicating the presence of organic modification)	–	1564	1553
Si–O stretching (longitudinal mode; shoulder of absorption band)	1115	1115	1115
In plane Si–O stretching	1030	1029	1030
In plane Si–O stretching	1006	1005	1006
OH deformation of inner hydroxyl groups	913	912	912
Si–O	789	789	790
Si–O, perpendicular	752	751	751

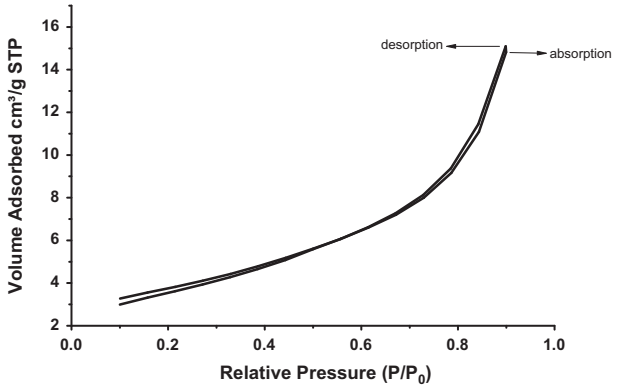

Figure 8 Adsorption isotherm of nitrogen on untreated Kaolin.

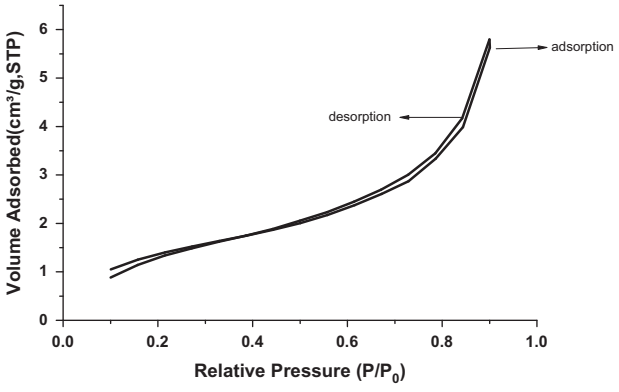

Figure 9 Adsorption isotherm of nitrogen on SRSO treated Kaolin.

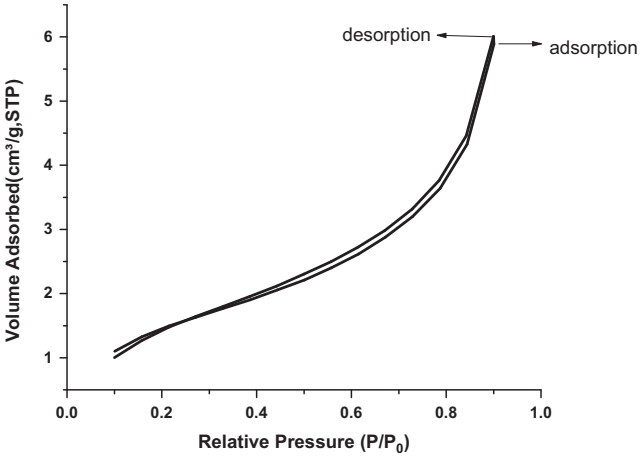

Figure 10 Adsorption isotherm of nitrogen on STSO treated Kaolin.

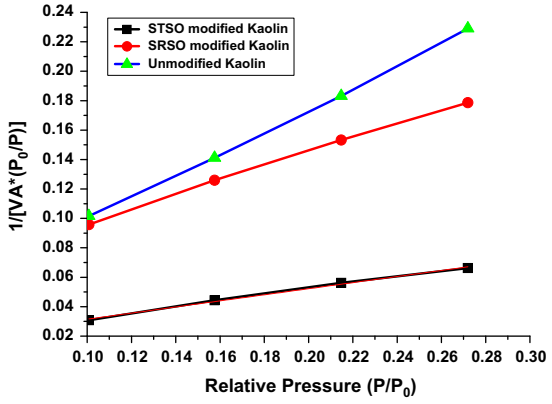

Figure 11 Langmuir plot of the different Kaolin samples.

lower compared to the value of 14.3 Å obtained by (Yahaya et al., 2010). The value of 13.40 Å recorded for SRSO treated Kaolin was low compared to the value of 14 Å obtained from an earlier study by Rugmini and Menon (2008) and high compared to the values of 12.5 Å and 12.6 Å obtained for sodium montmorillonite by Arroyo et al. (2003) and Wu et al. (2005), respectively.

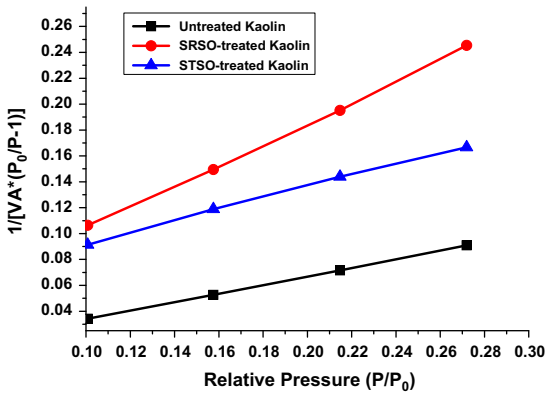

Figure 12 BET surface area plot for the Kaolin samples.

3.2. SEM studies

The SEM morphologies of untreated Kaolin, SRSO treated Kaolin and STSO treated kaolin are shown in Figs. 2–4. A closer look at the micrograph of the pristine kaolin in Fig. 2 reveals the hexagonal shape of the kaolinite crystal. The morphology of the kaolinite crystal is platelet shaped. In Fig. 3 the SRSO-treated kaolin has a compact plate-like farinaceous morphology which shows the presence of organic material (organomodification) in the kaolin. The SRSO treated kaolin has delaminated layers indicating an intercalation with organic material.

The STSO treated morphology in Fig. 4 clearly revealed the presence of organic material in the kaolin matrix. The STSO treated kaolin has delaminated layers indicating an intercalation with organic material.

3.3. FTIR studies

The FTIR spectra of untreated Kaolin, SRSO modified Kaolin and STSO modified kaolin are depicted in Figs. 5–7. The complete assignment of the absorption bands in measured IR spectra is summarized in Table 1. The unmodified as well as modified kaolins exhibited bands at 3620 cm^{-1} and 3654 cm^{-1} which are characteristics of inner hydroxyls (Vaculikova et al., 2011; Yahaya et al., 2010; Dai and Huang; 1999; Johnston and Stone, 1990) and hence are not accessible for interaction with guest molecules. In the case of organomodified samples, the occurrence of bands between 2850 cm^{-1} and 2920 cm^{-1} showed the occurrence of intercalation of SRSO and STSO on kaolin surfaces (Rugmini and Menon, 2008). These bands are attributed to the symmetric and asymmetric $–CH_2–$ stretching vibrations, respectively. In the treated samples, there is occurrence of bands between 1564 cm^{-1} and 1553 cm^{-1} showing the occurrence of intercalation of SRSO and STSO on kaolin surfaces which are attributed to C═O stretching. This intercalation process decreased the electrostatic attraction between the lamellae by causing an increase in the dielectric constant when the compounds penetrated between the layers. The sharp band at around 912 cm^{-1} and the weak shoulder at 940 cm^{-1} are due to the Al(VI)-OH vibrations.

3.4. The N_2 adsorption–desorption report

Surface area of all the samples under study was evaluated by employing nitrogen adsorption–desorption method. The pore volume and pore diameter were evaluated from the adsorption arm of isotherm based on Barrett–Joyner–Halenda (BJH) model. All the materials yielded a type IV isotherm as shown in Figs. 8–10 for the untreated kaolin, SRSO treated kaolin and STSO treated kaolin. Fig. 11 is the Langmuir plot of the samples investigated, while Fig. 12 is the BET surface area plot of the samples investigated. A summary of the results generated from the nitrogen adsorption–desorption experiment is shown in Table 2.

The reduction in surface areas, pore volumes and pore sizes of the SRSO treated and STSO treated kaolins is an indication of the formation of nanosized materials from kaolin (i.e. Nanoclay) which is a result of the organomodification process.

4. Conclusions

From the present study, the following conclusions were made:

1. The SRSO treated and STSO treated kaolins were intercalated as evidenced from an increased interlayer basal spacing in the X-ray studies and the C═O stretching from FTIR studies indicating the presence of organic modification at bands 1564 cm^{-1} and 1553 cm^{-1} for the SRSO and STSO modified kaolins, respectively.
2. New mesoporous materials from kaolin were synthesized and developed from oleochemicals.

Table 2 Summary report of the nitrogen adsorption/desorption properties of untreated, SRSO treated and STSO treated Kaolins.

Properties	Untreated Kaolin	SRSO treated Kaolin	STSO treated Kaolin
Area (m^2/g)			
Single point surface area at P/P_0 (0.272)	13.0179	4.8264	5.1747
BET surface area	13.1160	5.2287	5.6733
Langmuir surface area	21.0305	9.0155	9.9300
BJH adsorption cumulative surface area of pores between 17 Å and 3000 Å diameter	14.1274	5.12166	5.7424
Volume (cm^3/g)			
BJH adsorption cumulative pore volume of pores between 17 Å and 3000 Å diameter	0.023573	0.008447	0.008824
Pore size (nm)			
BJH adsorption average pore diameter (4 V/Å)	6.674	6.591	6.146

3. All the adsorption isotherms were found to conform to the Langmuir equation.
4. The adsorption isotherms of the modified kaolins were found to have the characteristic features of type IV isotherm according to IUPAC classification with initial part of the isotherm attributed to monolayer-multilayer adsorption.
5. The presence of hysteresis in all the isotherms indicates capillary condensation in the micropores.
6. The Single Point surface area, BET surface area, Langmuir surface area, External surface area, micropore area, and BJH adsorption cumulative surface area values of samples obtained by nitrogen adsorption were found to decrease in the following order: untreated (pristine) kaolin > STSO treated kaolin > SRSO treated kaolin.
7. The micropore volume and BJH adsorption cumulative pore volume values of samples obtained by nitrogen adsorption were found to decrease in the following order: untreated kaolin > STSO treated kaolin > SRSO treated kaolin.
8. The BJH Adsorption average pore diameter (4 V/Å) values of samples obtained by nitrogen adsorption were found to decrease in the following order: untreated kaolin > SRSO treated kaolin > STSO treated kaolin.
9. The pore sizes of the kaolin and the modified kaolin are within the mesoporous materials range of 2–50 nm with kaolin having a pore size of 6.674 nm > SRSO treated kaolin having 6.591 nm > STSO treated kaolin having 6.146 nm.

References

Arroyo, M., Lopez-Manchado, M.A., Herrero, B., 2003. Organomontmorillonite as substitute of carbon black in natural rubber compounds. Polymer 44, 2447–2453.

Ciullo, P.A., 1996. Industrial Minerals and Their Uses: A Handbook and Formulary. Noyes Publications, NJ, USA.

Dai, J.C., Huang, J.T., 1999. Surface modification of clays and clay–rubber composites. Applied Clay Science 15, 51–65.

Guessoum, M., Nekkaa, S., Fenouillot-Rimlinger, F., Haddoui, N., 2012. Effects of kaolin surface treatments on the thermomechanical properties and on the degradation of polypropylene. International Journal of Polymer Science. doi:10.1155/2012/549154.

Inel, O., Tumsek, F., 2000. The measurement of surface areas of some silicates by solution adsorption. Turkish Journal of Chemistry 24, 9–19.

Johnston, C.T., Stone, D.A., 1990. Influence of hydrazine on the vibrational modes of kaolinite. Clays and Clays Minerals 38, 121–128.

Krishnan, A.K., George, T.S., Anjana, R., Joseph, N., George, K.E., 2012. Effect of modified kaolin clays on the mechanical properties of polypropylene/polystyrene blends. Journal of Applied Polymer Science 127 (2), 1409–1415. doi:10.1002/app.38043.

Ma, X., Bruckard, W.J., 2010. The effect of pH and ionic strength on starch–kaolinite interactions. International Journal of Mineral Processing 94, 111–114.

Murray, H.H., 2007. Applied Clay Mineralogy: Occurrences, Processing and Application of Kaolins, Bentonites, Palygorskite–Sepiolite and Common Clays, first ed. Elsevier, Amsterdam.

Preetha, N.K., Rani, J., 2012. Nanokaolin clay as reinforcing filler in nitrile rubber. International Journal of Scientific and Engineering Research 3, 3.

Reichenauer, G., Scherer, G.W., 2001. Nitrogen sorption in aerogels. Journal of Non-Crystalline Solids 285, 167–174.

Rugmini, S., Menon, A.R.R., 2008. Organomodified kaolin as filler for natural rubber. Journal of Applied Polymer Science 107, 3476–3483.

Sing, K., 2001. The use of nitrogen adsorption for the characterization of porous materials. Colloids and Surfaces A: Physicochemical and Engineering Aspects 187–188, 3–9.

Songfang, Z., Shangchang, Q., Yuying, Z., Lei, C., Yong, G., 2011. Synthesis and characterization of kaolin with polystyrene via in-situ polymerization and their application on polypropylene. Materials and Design 32, 957–963.

Vaculikova, L., Plevova, E., Vallova, S., Koutnik, I., 2011. Characterization and differentiation of kaolinites from selected Czech deposits using Infrared spectroscopy and differential thermal analysis. Acta Geodynamics et Geomaterialia 8, 59–67.

Wang, H., Li, C., Peng, Z., Zhang, S., 2011. Characterization and thermal behaviour of kaolin. Journal of Thermal Analysis and Calorimetry 105, 157–160. doi:10.1007/s10973-011-1385-0.

Wu, Y.-P., Wang, Y.-Q., Zhang, H.-F., Wang, Y.-Z., Yu, D.-S., Zhang, L.-Q., Yang, J., 2005. Rubber- pristine clay nanocomposite prepared by co-coagulating rubber latex and clay aqueous suspension. Compos Sci. Technol 65, 1195.

Yahaya, L.E., Adebowale, K.O., Olu-Owolabi, B.I., Menon, A.R.R., Rugmini, S., Chameswary, J., 2010. Natural rubber/organoclay nanocomposites: effect of filler dosage on the physicomechanical properties of vulcanizates. African Journal of Pure and Applied Chemistry 4 (4), 198–205.